buildings

MDPI

Article

Correlation Analysis of Thermal Comfort and Landscape Characteristics: A Case Study of the Coastal Greenway in Qingdao, China

Yu Cong [1], Ruirui Zhu [1,*], Lei Yang [1], Xiaotong Zhang [1], Yibin Liu [1], Xi Meng [1,2] and Weijun Gao [1,2,3,*]

1 College of Architecture and Urban Planning, Qingdao University of Technology, Qingdao 266033, China; royalcicero@hotmail.com (Y.C.); yl18106369219@163.com (L.Y.); wfzhangxiaotong@163.com (X.Z.); l724052177@gmail.com (Y.L.); mengxihvac@163.com (X.M.)
2 Innovation Institute for Sustainable Maritime Architecture Research and Technology, Qingdao University of Technology, Qingdao 266033, China
3 Faculty of Environmental Engineering, The University of Kitakyushu, Kitakyushu 808-0135, Japan
* Correspondence: zhuruirui@qut.edu.cn (R.Z.); gaoweijun@me.com (W.G.)

Abstract: With the acceleration of urbanization throughout the world, climate problems related to climate change including urban heat islands and global warming have become challenges to urban human settlements. Numerous studies have shown that greenways are beneficial to urban climate improvement and can provide leisure places for people. Taking the coastal greenway in Qingdao as the research object, mobile measurements of the microclimate of the greenway were conducted in order to put forward an evaluation method for the research of outdoor thermal comfort. The results showed that different vegetation coverage affected the PET (physiologically equivalent temperature), UTCI (Universal Thermal Climate Index) as well as thermal comfort voting. We found no significant correlation between activities, age, gender, and thermal comfort voting. Air temperature sensation and solar radiation sensation were the primary factors affecting the thermal comfort voting of all sections. Otherwise, within some sections, wind sensation and humidity sensation were correlated with thermal sensation voting and thermal comfort voting, respectively. Both PET and UTCI were found to have a negative correlation with the vegetation coverage on both sides of the greenway. However, the vegetation coverage had positive correlation (R = 0.072) for thermal sensation and significant positive correlation (R = 0.077*) for thermal comfort. The paved area cover was found to have a positive correlation with PET and UTCI, while having a negative correlation with thermal sensation (R = −0.049) and thermal comfort (R = −0.041). This study can provide scientific recommendations for the planning and design of greenway landscapes to improve thermal comfort.

Keywords: outdoor thermal comfort; microclimate; greenway; mobile measurement

check for updates

Citation: Cong, Y.; Zhu, R.; Yang, L.; Zhang, X.; Liu, Y.; Meng, X.; Gao, W. Correlation Analysis of Thermal Comfort and Landscape Characteristics: A Case Study of the Coastal Greenway in Qingdao, China. *Buildings* **2022**, *12*, 541. https://doi.org/10.3390/buildings12050541

Academic Editors: Bo Hong, Yang Geng and Dayi Lai

Received: 22 March 2022
Accepted: 21 April 2022
Published: 24 April 2022

1. Introduction

Climate problems caused by climate change including the urban heat island (UHI) effect [1] and global warming have become global issues in human settlements with the acceleration of urbanization around the world. Numerous studies [2–4] have established that UHIs can jeopardize the thermal comfort and health of urban residents. Climate change has reduced people's willingness to engage in outdoor public activities, but their desire for access to nature has not diminished. Coastal cities face the same problems of UHIs and extreme climates as inland cities. Based on this background, scholars [5–7] have started to conduct climate studies in coastal cities, however, urban planners still face a lack of scientific evidence for landscape and urban planning in the built environment due to a lack of the comprehensive evaluation of thermal comfort.

Greenways have been regarded as a critical natural resource for enhancing the quality of the built environment and alleviating urban climate issues including UHIs [8–12]. Therefore, they were developed in response to urban climate concerns and the dearth of public space in cities as they can connect nature and human settlements to help resolve environmental problems [13–16].

In China, the research of greenways is in its infancy. Current research on coastal greenways in China tend to focus on the southern coastal provinces with a subtropical monsoon climate such as Guangdong Province. For example, J. Y. Wu et al. [17,18] evaluated the Guangdong Zengcheng Greenway and analyzed the design strategy of its agricultural landscapes. L. P. Hong et al. [19] studied the Guangdong Dongguan Greenway as a new path to explore coordinated urban–rural development under the low-carbon model. Z. Liu et al. [20] investigated the greenway planning in the Pearl River Delta region of Guangdong. W. X. Chi [21] researched the use of community greenways in high-density residential areas in Guangzhou. However, most of the above studies mainly focused on the design and planning strategies or ecological and landscape evaluation of greenways in coastal cities, and paid less attention to the microclimate of greenways, which can influence human thermal comfort to a very large extent. In addition to the above, coastal cities in northern China also have a suitable environment for the construction of greenways, but greenways are less developed compared to southern cities, while relevant research and case studies are insufficient.

Moreover, it is difficult to define effective microclimatic regulation strategies for all applications because of the particular characteristics of various cities. Therefore, in this study, we chose a coastal greenway in Qingdao, Shandong Province, a coastal city in northern China with an oceanic temperate monsoon climate, as the research object. The study aimed to present an evaluation method of microclimate and outdoor thermal comfort through measurements of the microclimate of the pedestrian walkway and its surrounding landscape. By applying the correlation analysis of outdoor thermal comfort and landscape characteristics, the study can provide scientific recommendations for the planning and design of greenways as well as guidance for the construction of urban coastal greenways in the northern coastal cities of China, and even similar climatic zones around the world.

Currently, the most commonly used microclimate measurement method is fixed weather stations, but it also presents limitations associated with the demand for a large number of equipment and operators to acquire the data synchronously. The mobile measurement (also known as the mobile observation method or the mobile survey) is a measurement method that has used in the field of urban meteorology to study the urban heat island effect and urban microclimate in recent years [22,23]. A. Sundburg [24] first invented it when he conducted an empirical study of heat island intensity. A. Qaid et al. [25] also conducted the mobile measurement in order to investigate the UHI phenomenon and outdoor thermal comfort on a micro-scale in various areas of a planned city. S. A. Zaki et al. [26] used a motorcycle equipped with a datalogger to conduct mobile measurements within the target area at night in order to investigate the urban morphological impact of Kampung Bara on the UHI. S. Tondini et al. [27] demonstrated a low-cost cloud-connected mobile monitoring platform for urban microclimate data. S. Y. Chan et al. [28] used mobile measurements to study the effects of microclimate and thermal comfort in urban parks. B. J. He et al. [29] studied the precinct ventilation and its associated influences on UHI effects and outdoor thermal comfort via the mobile measurement. Thus, these studies confirmed the validity of mobile measurements for UHI, microclimate, and thermal comfort studies in urban outdoor spaces including urban parks, communities, micro-scale urban spaces, etc. Taking into account the features of the selected cases, the mobile measurement was used for the microclimate data collection in this study.

PET (physiologically equivalent temperature) and UTCI (Universal Thermal Climate Index) are objective outdoor thermal comfort indicators widely used internationally. PET is the physiologically equivalent temperature based on the two-node model in a given environment, and its value is equal to the temperature corresponding to the outdoor equivalent thermal state under typical indoor conditions [30]. UTCI is a climate index developed by the International Society for Biometeorology based on the multi-point thermal regulation model by Fiala, which can be used for extreme climate forecasting and urban climate studies [31]. In recent years, many studies [32–36] have found that they can be effectively applied in several outdoor thermal comfort studies in Asian countries and regions including China. For these reasons, PET and UTCI were chosen as the main objective outdoor thermal comfort indexes in this paper, and were calculated by the software Rayman Pro [37] based on the measured microclimate data (Appendix A).

2. Methods

2.1. The Site

2.1.1. Climatic Background of the City

The research was conducted on the Laoshan District Coastal Walkway in Qingdao City, Shandong Province, People's Republic of China. Qingdao is a coastal city in China, located in the southeast of the Shandong Peninsula (Figure 1). It has a maritime temperate monsoon climate. As a coastal city, Qingdao's climate is strongly influenced by the sea, with humid air, abundant rainfall, moderate temperatures, and distinct seasons. Its annual average temperature is approximately 12 degrees, and its annual average rainfall is approximately 660 mm. From July to September, the climate is relatively warm, with August being the hottest month of the year, with an average whole-day temperature of 27.5 degree (Figure 2). In comparison to other inland areas of China, Qingdao is cooler in the summer, with few days exceeding 30 degrees, but due to the high humidity, residents here feel muggy. As a result, the study focused primarily on the microclimate and thermal comfort of people on the greenway during the summer.

Figure 1. The map of Qingdao City, Shandong Province, People's Republic of China.

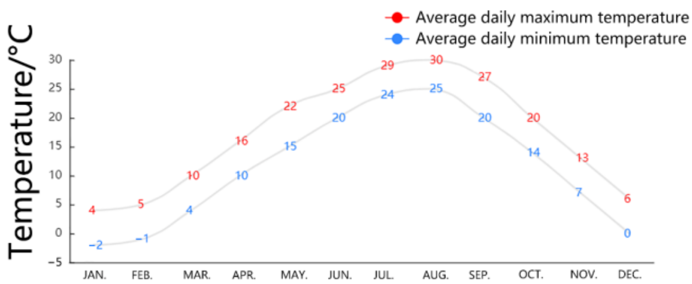

Figure 2. The meteorological analysis chart of monthly average temperature in Qingdao in 2021 (the meteorological information is cited from the Qingdao Meteorological Bureau).

2.1.2. The Measured Site

The Qingdao Coastal Recreation Walkway System spans the two administrative districts of Shinan and Laoshan in Qingdao City, beginning at Tuandao Ring Road in the west and ending at Shilaoren Beach in the east. With a total length of approximately 36.9 km, it connects Badaguan Scenic Area, May Fourth Square, Shilaoren Beach, and other major tourist attractions in Qingdao; the Laoshan District Coastal Walkway is an integral part of the Qingdao Coastal Recreation Walkway System, with a total length of approximately 8 km. It begins in the west at Yinhai Amusement Park and ends in the east at Shilaoren Beach (Figure 3). From a functional standpoint, the Laoshan District Coastal Walkway can be defined as a coastal recreational greenway in Qingdao, as it is located on the Qingdao coastline and utilizes the landscape and slow walking trail system to connect important tourist and leisure attractions along the Laoshan District's coast.

Figure 3. The plan of the section from Maidao Road to Haiyou Road of the Laoshan District Coastal Walkway.

In this study, we selected the Maidao Road to Haiyou Road section as the specific measured object because it is 1.5 km long, has the highest pedestrian flow, and is the most representative and richer landscape node type in the Laoshan District Coastal Walkway (Figure 3). Simultaneously, the selected sample plots were subdivided into nine sample sections denoted by the letters A to I, according to the different landscape nodes, and the microclimate parameters were investigated using field measurements.

The measured site was divided into nine sections, numbered from A to I, based on the location of various landscape nodes (Figure 4). Section A is adjacent to Maidao Road and serves as the entrance, which is densely forested and offers numerous recreational opportunities. Section B is a Miscanthus trail, with a predominance of ornamental grasses. Section C is a seaside square with less vegetation and a heavy reliance on hard pavement. Section D is a shrub trail with a predominance of dwarf shrubs. Section E is a trestle bridge over the sea; the site is devoid of vegetation and primarily composed of wood pavement. Section F is a soil slope landscape area characterized by undulating terrain and sparse vegetation cover. Section G is a reef landscape area, with gravel and reefs dominating the site. Section H is a sparse forest and grassland with an open visual field and abundant vegetation. Section I is a recreational plaza that is lightly vegetated, with recreational pavilions and other service facilities located throughout the site.

According to the field visit and the Google satellite map of the site, we calculated the vegetation coverage ratio [38] and the paved area coverage ratio by using the measurement function of the software AutoCAD and ArcGIS (Table 1).

Figure 4. The photo of Section A to Section I.

Table 1. Vegetation coverage, and paved area coverage of each section.

Section No.	A	B	C	D	E	F	G	H	I
Vegetation Coverage	0.578	0.896	0.192	0.530	0.130	0.400	0.450	0.400	0.300
Paved Area Coverage	0.422	0.104	0.808	0.470	0.870	0.536	0.402	0.600	0.700

2.2. Microclimate Measurements

2.2.1. Date, Time, and Specific Methods of Measurement

Summer in Qingdao typically lasts from July through September. Based on our pre-survey and visits to the selected site, we found that the number of visitors to the site is higher in early September, since the colleges nearby start their new academic year in September, which means that more interviewees can be recruited. Therefore, according to the city's climate, the pre-survey of the selected site and the situation of visitors, we chose to conduct the experiment on 11 September (Saturday) and 12 September 2021 (Sunday). Meanwhile, by observing the frequency of people using the greenway throughout the day in the pre-survey, 9:00 and 9:30, 12:00 to 12:30, and 16:00 to 16:30 were chosen as the specific experimental times.

On the day of measurement, a researcher was set up with dataloggers and a GPS device to collect microclimatic parameters along a pre-planned route of 1.5 km (Figure 5) including air temperature, relative humidity, wind speed, and solar radiation. Throughout the mobile survey, the researcher moved at a uniform speed during the selected time period (9:00 to 9:30, 12:00 to 12:30, and 16:00 to 16:30), in order to investigate the changes in the microclimatic parameters under different sections of the site at the three time periods. In this study, the researcher conducted the measurements in each section (A to I) consecutively, and cluster analysis [39] was performed on the original data in order to reduce errors.

2.2.2. Measurement Equipment

Microclimate weather data were collected using the Kerel 5500 handheld weather station and the TES-1333R solar power meter (Figure 6), and the researcher dynamically monitored changes in air temperature, humidity, wind speed, and solar radiation at a height of 1.5 m above the ground. The TES-1333R solar power meter features automatic data access and is compatible with RS232 data transmission. Additionally, the researcher wore a GPS positioning device or carried and activated the GPS positioning service function on a smart phone during the actual measurement, and recorded the actual measured movement path and GPS positioning data in real-time. All instruments were set to switch on and off automatically at the same time, and to store data automatically every 2 s in advance. Table 2 shows the equipment's specifications as well as its main parameters.

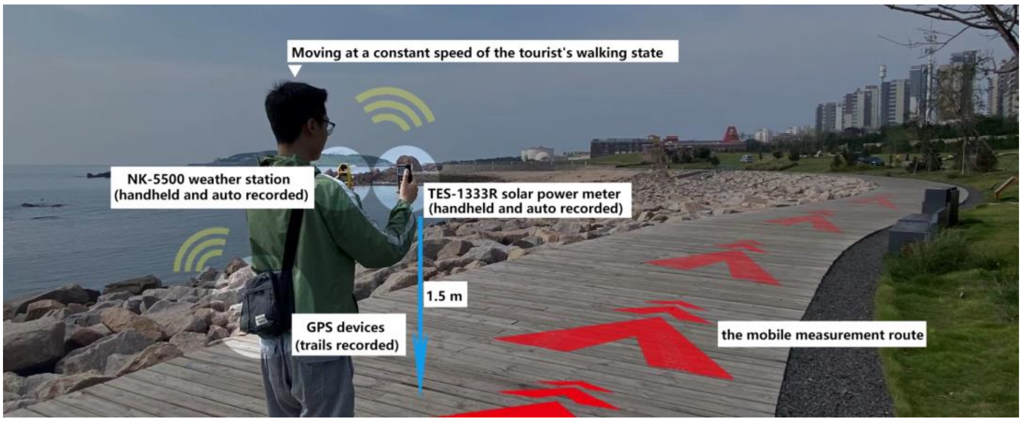

Figure 5. A researcher monitoring microclimate meteorological data in the Laoshan District Coastal Walkway.

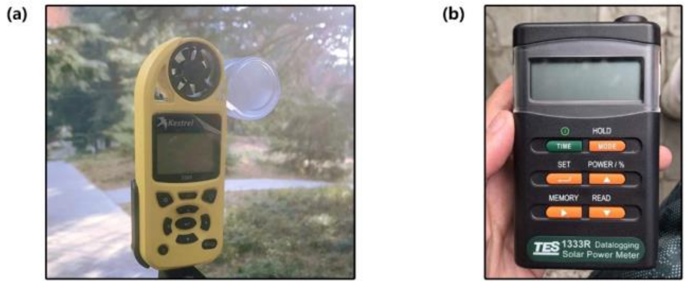

Figure 6. The photo of the Kerel 5500 handheld weather station (**a**) and the TES-1333R solar power meter (**b**).

Table 2. Specification of the equipment.

Name	Storage Method	Parameter	Accuracy	Test Range	Unit	Data Output
Kerel NK-5500 handheld weather station	Manual or Automatic	Air temperature	±1.0	−29~70	°C	The screen displays stable data and records automatically.
		Relative humidity	±3	0~100.0	%	
		Wind speed	±3	0.1~60.0	m/s	
TES-1333R solar power meter	Manual or Automatic	Solar radiation	±10	0~2000	W/m^2	The screen displays stable data and records automatically.

2.3. Questionnaire Survey

The questionnaire used in this survey (Appendix C) consisted of three parts. The first part included the date, time, and place of investigation, which was marked at the top of the questionnaire and filled in by the interviewer. The second part included the interviewee's gender, age, dress, and the main purpose of coming to the place. The information about the interviewee's dress included a top, bottom, and shoes. All the information was obtained by the interviewer through observation and oral inquiry. The last part was the content related to human thermal sensation and human thermal comfort, which included six questions. Question No. 1 was the thermal sensation vote, which was divided into seven options according to the ASHRAE seven-point scale including cold, cool, slightly cool, neutral, slightly warm, warm, and hot. Question No. 2 was the thermal comfort vote with five options, namely, unbearable, uncomfortable, slightly uncomfortable, and comfortable. Interviewees were asked to mark the corresponding options based on their instant thermal sensation and thermal comfort. Questions Nos. 3 to 6 were the sensation vote for the air temperature, relative humidity, wind speed, and solar radiation.

While a researcher was conducting physical measurements, one volunteer was arranged in each section from section A to section I (nine volunteers in total) to record the basic information and real-time subjective thermal comfort such as thermal sensation, thermal comfort, temperature sensation, wind sensation, humidity sensation, and solar radiation sensation of the visitors in each section by the questionnaire survey. In the study, the interview data was sorted by MS Excel and analyzed in SPSS software.

3. Results

3.1. Microclimate Analysis

3.1.1. Temperature Analysis

Figure 7 shows that, in general, the air temperature of the place rose first and then fell with time changes. The lowest temperature was recorded during 16:00 and 16:30, and the highest was recorded during 12:00 and 12:30. In term of spatial change, from 12:00 to 12:30, the air temperature decreased sharply in Section B and Section F. Additionally, the air temperature decreased in Section H during 12:00 and 12:30 on 11 September, but did not decrease on 12 September.

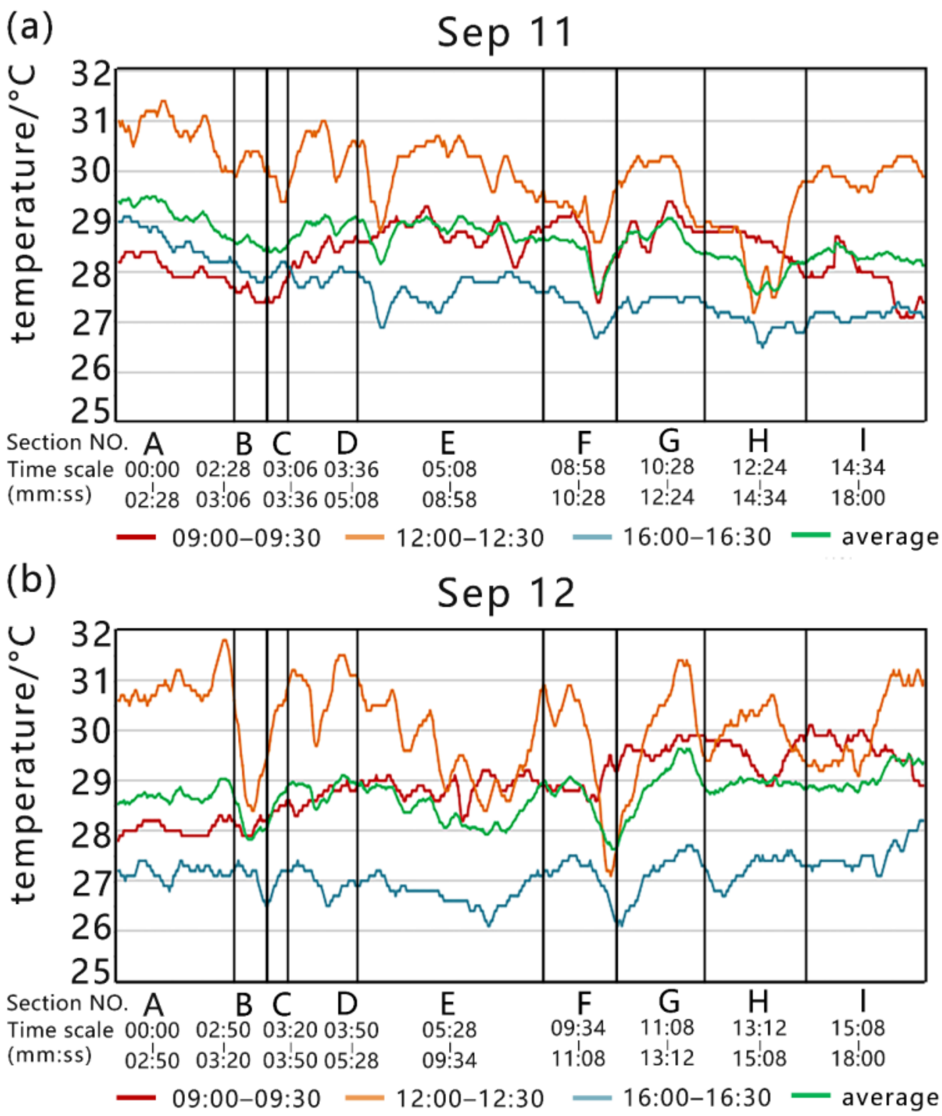

Figure 7. The line charts depicting the air temperature changes over three time periods on 11 September (**a**) and 12 September (**b**).

3.1.2. Relative Humidity Analysis

Figure 8 shows that, in terms of time change, the relative humidity of the location generally showed a trend of first decreasing and then increasing on both days. In terms of spatial change, for 11 September, the average humidity fluctuated by less than 6%, and the lowest average humidity was 75% in Section E, and the highest was 80% in Section H. For 12 September, the average relative humidity fluctuated by around 6%, with Section I having the lowest average relative humidity at 70%. However, the highest average humidity was found in Section G, where it was 76%.

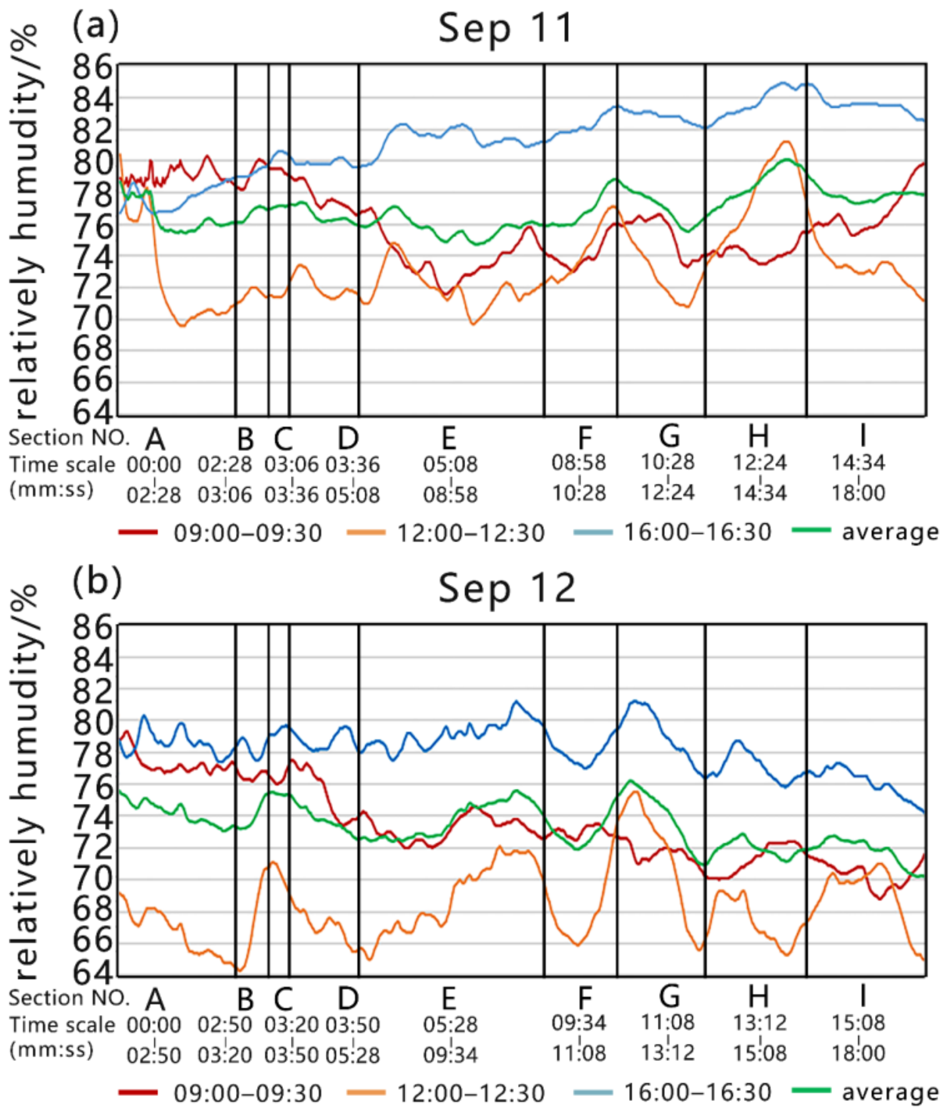

Figure 8. The line charts depicting the relative humidity changes over three time periods on 11 September (**a**) and 12 September (**b**).

3.1.3. Wind Speed Analysis

Figure 9 shows that the overall wind speed threshold on 11 September was 0–2.0 m/s, while the wind speed on 12 September was faster in general, with a threshold of 0–3.9 m/s. The maximum wind speed on both 11 September and 12 September occurred between 16:00 and 16:30. In terms of spatial change, the maximum average wind speed on 11 September occurred between the junction of Sections G and H at 1.36 m/s, while the maximum average wind speed on 12 September occurred between the junction of Sections B and C at 2.66 m/s.

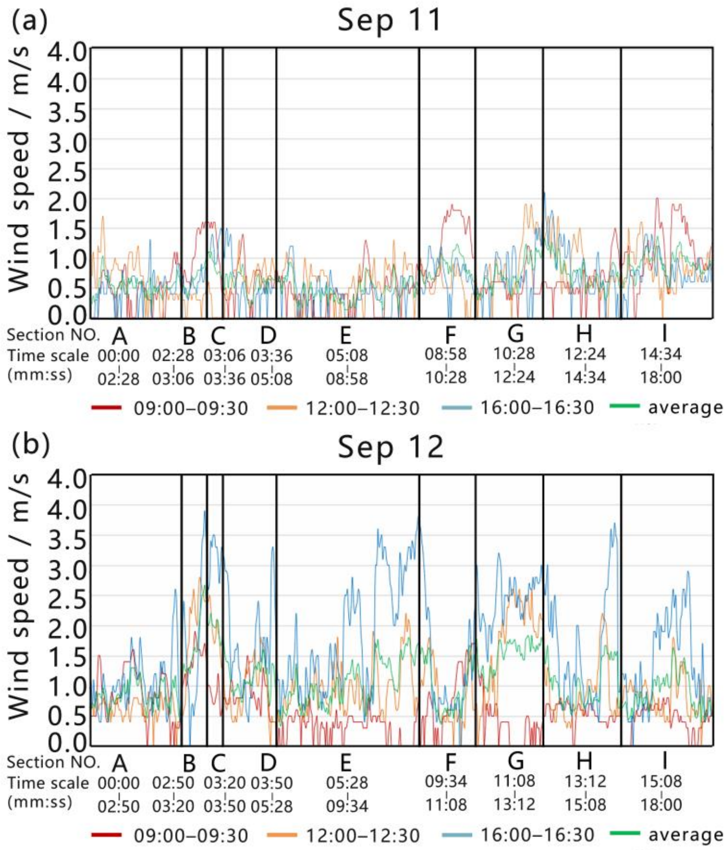

Figure 9. The line charts depicting the wind speed changes over three time periods on 11 September (**a**) and 12 September (**b**).

3.1.4. Solar Radiation Analysis

Figure 10 shows that the average solar radiation of 9:00 to 9:30 and 12:00 to 12:30 on 11 September and 12 September were both higher than the average solar radiation of 16:00 to 16:30, and the solar radiation on both days showed a trend of rising and then falling in terms of time variation. The solar radiation from 12:00 to 12:30 on 11 September fluctuated from Section C to Section F due to cloud cover, so the average solar radiation from 12:00 to 12:30 on 11 September was slightly lower than its value from 9:00 to 9:30. However, the field was not affected by clouds on 12 September from 12:00 to 12:30, thus the average solar radiation in this time period was the highest. In terms of spatial variation, the solar radiation in the Section H from 12:00 to 12:30 was the highest value on 11 September, and the solar radiation in the Section G from 12:00 to 12:30 was the highest value on 12 September.

3.1.5. Interaction between the Measured Microclimate Parameters

We performed Spearman correlation analysis among the measured microclimate parameters. According to Table 3, we found that all four parameters were correlated with each other significantly in this study.

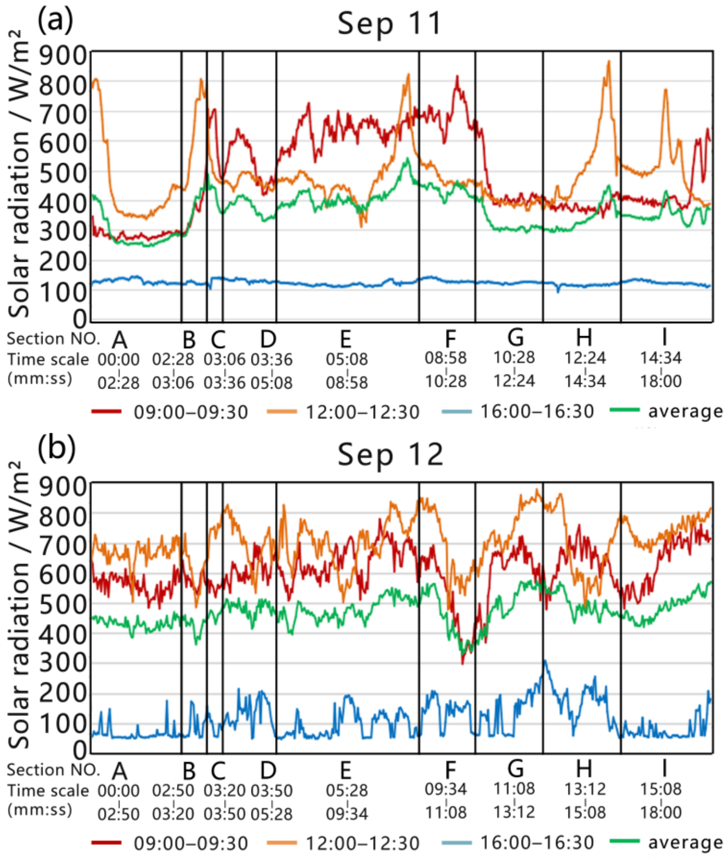

Figure 10. The line charts depicting the solar radiation changes over three time periods on 11 September (**a**) and 12 September (**b**).

Table 3. The Spearman correlation analysis of measured parameters.

	Spearman	Air Temperature	Relative Humidity	Wind Speed	Solar Radiation
Air Temperature	R.	/	−0.855 **	−0.243 **	0.687 **
	S.	/	0.000	0.000	0.000
Relative Humidity	R.	−0.855 **	/	0.41 *	−0.719 *
	S.	0.000	/	0.013	0.000
Wind Speed	R.	−0.243 **	−0.41 *	/	−0.101 **
	S.	0.030	0.013	/	0.000
Solar Radiation	R.	−0.687 **	−0.719 **	−1.01 **	/
	S.	0.000	0.000	0.000	/

Notes: R. refers to the correlation coefficient while S. refers to the significance index, which reflect the correlation and the significance of the correlation. * At the 0.05 level (two-tailed), the correlation is significant. ** At the 0.01 level (two-tailed), the correlation is significant.

3.2. Objective Thermal Comfort Surveys

3.2.1. Correlation Analysis of the Vegetation Coverage, the Paved Area Coverage with PET, UTCI

In this study, we correlated the vegetation coverage with the PET and UTCI of each section (Figure 11). The conclusion (Table 4) reflects that the vegetation coverage area on both sides of the greenway showed a certain negative correlation with its PET and UTCI, in which the vegetation coverage rate was significantly correlated with PET from 12:00 to 12:30 and with UTCI from 16:00 to 16:30.

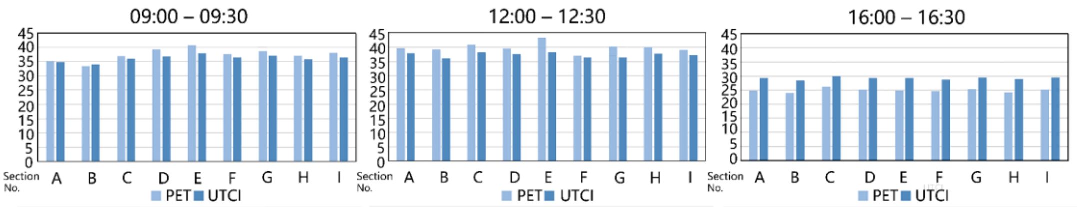

Figure 11. The PET and UTCI for different sections during the three time periods.

Table 4. The Spearman correlation coefficients of the vegetation coverage and PET&UTCI.

09:00–09:30				12:00–12:30				16:00–16:30			
Spearman		**PET**	**UTCI**	**Spearman**		**PET**	**UTCI**	**Spearman**		**PET**	**UTCI**
Vegetation Coverage	R. S.	−0.494 0.177	−0.510 0.160	Vegetation Coverage	R. S.	−0.326 * 0.391	−0.552 0.123	Vegetation Coverage	R. S.	−0.647 0.06	−0.706 * 0.034

* At the 0.05 level (two-tailed), the correlation was significant.

Additionally, correlation analysis was performed between the paved areas and PET and UTCI. In contrast to the situation between vegetation coverage and PET and UTCI, the paved area ratio was positively correlated with PET and UTCI in all time periods, in which the paved area ratio was significantly correlated with UTCI during 12:00 and 12:30 (Table 5). According to Figure 11, Sections C (the hard paved plaza) and E (the hard paved trestle) with lower vegetation cover and higher pavement cover showed higher PET and UTCI values, while Sections A (the entrance) and B (the Miscanthus trail) with higher vegetation cover and lower pavement cover showed the opposite trend.

Table 5. The Spearman correlation coefficients of the paved areas ratio and PET and UTCI.

09:00–09:30				12:00–12:30				16:00–16:30			
Spearman		**PET**	**UTCI**	**Spearman**		**PET**	**UTCI**	**Spearman**		**PET**	**UTCI**
Paved Areas	R. S.	0.367 0.332	0.367 0.332	Paved Areas	R. S.	0.500 0.170	0.683 * 0.042	Paved Areas	R. S.	0.561 0.116	0.644 0.061

* At the 0.05 level (two-tailed), the correlation was significant.

3.2.2. Correlation Analysis of Measured Microclimatic Parameters with PET and UTCI

In this study, we correlated the measured microclimatic parameters with its PET and UTCI for each section in three different time periods. Additionally, the correlation analyses were based on the data of both days. The results (Tables 6–8) showed that the microclimatic parameters affecting PET and UTCI most at the sample site were different during different time periods. Between 09:00 to 09:30, the air temperature and the wind speed were the most significant parameters influencing PET, while the solar radiation was the most significant parameter influencing UTCI. From 12:00 to 12:30, the air temperature was the most significant parameters affecting both PET and UTCI. From 16:00 to 16:30, the wind speed was the most significant parameter affecting both PET and UTCI.

Table 6. The Spearman correlation coefficients of the measured microclimatic parameters and PET and UTCI of 09:00 to 09:30.

09:00–09:30					
	Spearman	**Air Temperature**	**Relative Humidity**	**Wind Speed**	**Solar Radiation**
PET	R. S.	0.717 * 0.030	−0.483 −0.035	−0.733 * 0.025	0.650 0.058
UTCI	R. S.	0.583 0.099	0.350 0.356	−0.633 0.067	0.783 * 0.013

* At the 0.05 level (two-tailed), the correlation was significant.

Table 7. The Spearman correlation coefficients of the measured microclimatic parameters and PET and UTCI of 12:00 to 12:30.

12:00–12:30					
	Spearman	**Air Temperature**	**Relative Humidity**	**Wind Speed**	**Solar Radiation**
PET	R.	0.633 *	−0.133	−0.483	0.550
	S.	0.067	−0.732	0.187	0.125
UTCI	R.	0.717 *	−0.117	−0.267	0.417
	S.	0.030	0.765	0.488	0.265

* At the 0.05 level (two-tailed), the correlation was significant.

Table 8. The Spearman correlation coefficients of the measured microclimatic parameters and PET and UTCI of 16:00 to 16:30.

16:00–16:30					
	Spearman	**Air Temperature**	**Relative Humidity**	**Wind Speed**	**Solar Radiation**
PET	R.	0.319	−0.226	−0.924 **	0.109
	S.	0.402	−0.035	0.000	0.058
UTCI	R.	0.395	−0.268	−0.966 **	−0.050
	S.	0.293	0.486	0.000	0.013

** At the 0.01 level (two-tailed), the correlation was significant.

3.3. Subjective Thermal Comfort Surveys

3.3.1. Analysis of Interviewees' Basic Information

A total of 900 questionnaires were distributed and 800 were collected, with 791 valid in this study. In this survey, young adults aged 26 to 34 accounted for half of all interviewees, followed by young college students aged 19 to 25 (Figure 12).

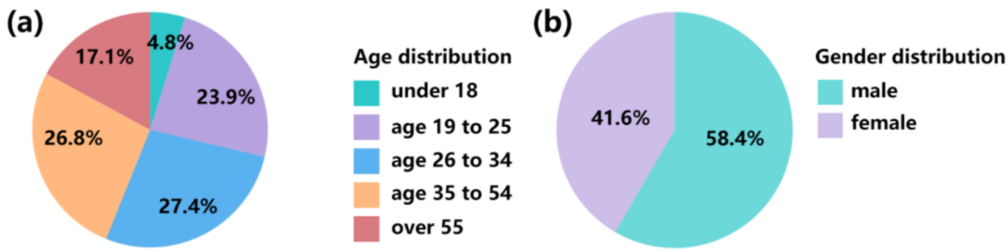

Figure 12. Tables displaying the age (**a**) and gender distribution (**b**) of interviewees.

People over the age of 55 made up 17.1% of the population. Observations revealed that 77.0% of interviewees wore short sleeves (or long skirts), 12.7% wore long sleeves, 7.6% wore thin coats, and 2.7% wore vests. At the same time, the research team discovered that 84.2% of the interviewees wore sneakers or leather shoes for activities, while the remaining 15.8% wore slippers or sandals.

3.3.2. Crowd Behavior and Activities Analysis

According to the questionnaire, the most popular times for interviewees to visit the place were 15:00–17:00 and 9:00–11:00, followed by 12:00–14:00, then 18:00, and 6:00–8:00. Notably, the interviewees' preferred time to visit the park also coincided with the time when the PET and UTCI were relatively low (the time period of 09:00–09:30 and 16:00–16:30), which is consistent with the previous results on PET and UTCI (Figure 13).

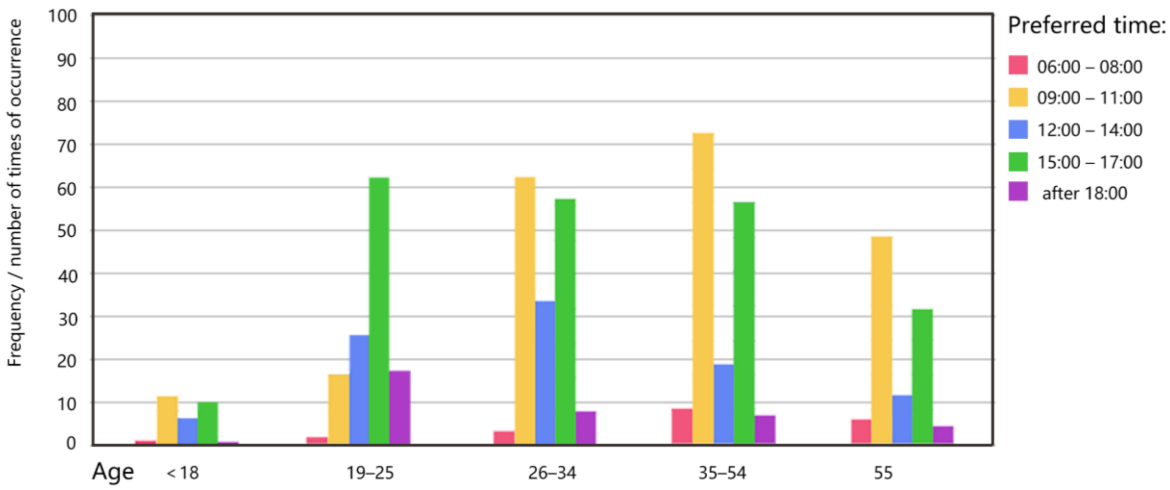

Figure 13. Frequency distribution of interviewees of different ages and their preferred time.

The research team analyzed the frequency distribution of the types of activities performed by the interviewees at various times using the questionnaire. Interviewees chose physical exercise such as walking and jogging as their main activities in the survey conducted during 9:00 to 9:30 on 11 September and 12 September. From 12:00 to 12:30, 48.1% of the interviewees chose to go on a leisurely tour, while 30.8% chose to go for a walk, and the remaining 21.1% chose other types of activities. During 16:00 and 16:30, 48.8% of interviewees went for a walk while 26.6% went on a leisure tour, and the remaining 24.6% chose other types of activities.

By analyzing interviewees of different ages and their preferred time, we found that interviewees under 25 years old preferred to come to the greenway around 15:00 to 17:00, while those over 25 years old, especially those aged 35 to 54 years old, preferred to choose 9:00 to 11:00. Additionally, we found that interviewees under 25 years old preferred to come to the greenway in order to tour for leisure, while those over 25 years old preferred to have a walk here (see Figure 14).

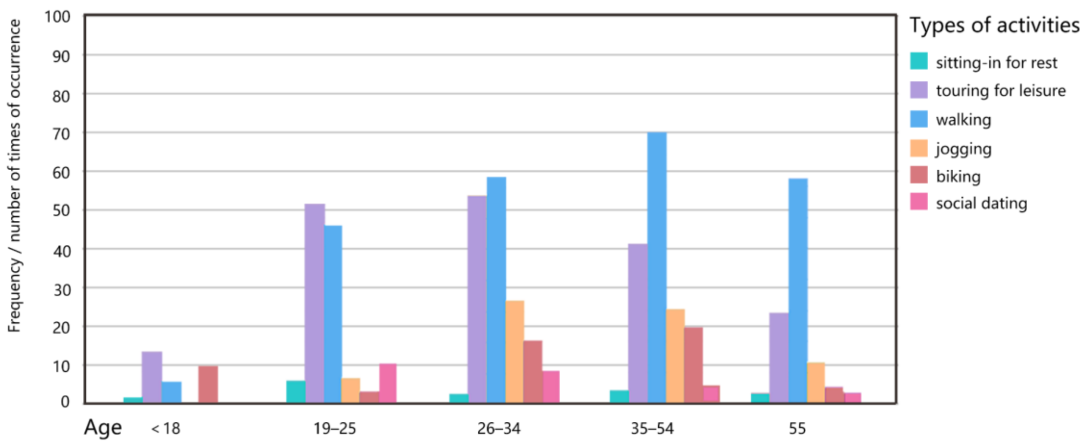

Figure 14. Frequency distribution of interviewees of different ages and their preferred activities.

3.3.3. Results of Sensation Votes and Thermal Comfort Votes

Detailed sensation votes and thermal comfort votes are shown in Appendix B. Due to force majeure factors, Section D was routinely maintained on the second experimental day, with few visitors for us to interview. Thus, unfortunately there was no data of thermal comfort and thermal sensation votes for 12 September, and the data on Section D presented here is for 11 September. In addition, we also found some anomalies that were not in line with common sense, so these anomalies were considered as an outlier and excluded from the sample after considering whether they were due to clothing, age, or personal reasons.

Correlation Analysis of Votes with Types of Activities, Age and Gender

According to the results of the thermal sensation votes and thermal comfort votes, we performed one-way ANOVA on the results of thermal sensation votes and thermal comfort votes with different types of activities and age, respectively, but since their variance homogeneity test failed, thermal sensation votes and thermal comfort votes of different activity types and different ages in the study were not statistically significant.

Additionally, after case weighting of the number of men and women, we performed the chi-square test on the results of the thermal sensation votes and thermal comfort votes with gender. Because the asymptotic significance was much higher than 0.05, there was no significant difference, which means that different gender had no significant effect on the thermal sensation votes and thermal comfort votes in this study.

Correlation Analysis of Vegetation Coverage, Paved Area Coverage with Thermal Sensation Votes, Thermal Comfort Votes

We conducted Spearman correlation analysis among the vegetation cover of each section and the thermal sensation votes. According to the results (Table 9), their Spearman correlation coefficients, although greater than zero, were much less than 0.30 (i.e., there was a weak positive correlation between vegetation cover and thermal sensation votes in this study).

Table 9. Spearman correlation of vegetation cover with thermal sensation and thermal comfort.

	Spearman	Thermal Sensation	Thermal Comfort
Vegetation Coverage	R.	0.072	0.077 *
	S.	0.055	0.038

* At the 0.05 level (two-tailed), the correlation was significant.

We also performed Spearman correlation analysis among the vegetation cover of each section and thermal comfort votes, and we found a significant positive correlation between vegetation cover and thermal comfort votes at the 0.05 level (two-tailed) (Table 9), which means that the higher the vegetation cover, the more the interviewees tended to be comfortable in that section.

Similarly, we performed correlation analysis between the paved area ratio and thermal sensation and thermal comfort. According to the findings (Table 10), a weak negative link existed between pavement cover and thermal sensation and thermal comfort votes in this study, in contrast to the situation with vegetation cover and thermal sensation and thermal comfort votes.

Table 10. Spearman correlation of the paved area ratio with thermal sensation and thermal comfort.

	Spearman	Thermal Sensation	Thermal Comfort
Paved Area	R.	−0.049	−0.041
	S.	0.190	0.268

4. Discussion

4.1. Summary of the Microclimate Measurement and Thermal Comfort Vote

According to the results, the microclimatic parameters changed the interviewees' votes on 11 September and 12 September. In terms of the change in time, the measured air temperature showed a trend of increasing and then decreasing, accordingly, the interviewees' perception of air temperature gradually tended to be "slightly high" from "neutral", and finally dropped back to "neutral". The measured wind speed was the strongest during 16:00 and 16:30, and the wind speed sensation vote tended to be "slightly strong" and "strong" in this time period. Moreover, the measured relative humidity was lowest from 12:00 to 12:30, and so accordingly, the measured relative humidity was weakest during 12:00 and 12:30, and the humidity sensation votes appeared "slightly dry" and "neutral" more often at this time period.

Additionally, the different vegetation cover and paved area cover in each section affected the PET, UTCI, and interviewees' thermal comfort votes in this study. Both PET and UTCI were found to have a certain negative correlation with the vegetation coverage on both sides of the greenway. Moreover, there was a weak positive correlation (R = 0.072) between the vegetation coverage and thermal sensation and a significant positive correlation (R = 0.077*) between the vegetation coverage and thermal comfort. In contrast, the paved area cover was found to have a positive correlation with PET and UTCI and a negative correlation with thermal sensation (R = −0.049) and thermal comfort (R = −0.041). In two adjacent sections, the one with the lower vegetation coverage and higher paved area cover had more extremes of air temperature and solar radiation than the one with the higher vegetation coverage. For instance, Section A, with the vegetation cover of 0.57 and paved area cover of 0.42, experienced higher average air temperature than Section B with the vegetation cover of 0.89 and paved area cover of 0.10. However, Section E with the vegetation coverage of 0.13 and paved area cover of 0.87 experienced higher average solar radiation than Section D, with the vegetation coverage of 0.53 and paved area cover of 0.47, and Section F, with the vegetation coverage of 0.40 and paved area cover of 0.53. Besides, other landscape factors such as the surface roughness, had a weakly negative effect on thermal sensation and thermal comfort in this study.

In addition, it was concluded that there was no significant effect of differences in the types of activities, age, and gender on thermal sensation and thermal comfort in this study.

4.2. Comparison with Previous Studies

Despite the experimental site for this study being a coastal greenway, which differed from prior studies of other urban outdoor space, some similar conclusions can be reached. Previous microclimate studies of other urban outdoor space revealed that spaces with larger canopy or higher crown plants had a regulating effect on the temperature of the outdoor green space [40,41]. In addition, a previous study also found that space with high vegetation coverage in urban parks could improve thermal comfort [42]. Section B is a Miscanthus trail, with a predominance of miscanthus plants and coniferous plants with higher crowns in the periphery, and the vegetation coverage was the highest. Therefore, the reason for the temperature decreasing here, and mentioned in the results, could be contributed to the changing climate conditions by the sea, plants with higher crowns, and higher vegetation coverage. For Section F, the reason for the decrease in temperature could be a soil slope landscape here, and the height of the surrounding landscape, which is bigger. Furthermore, previous research discovered that the height and slope of the surrounding landscape influenced the air and surface temperature nearby [43,44]. As a matter of fact, the average air temperature from 12:00 to 12:30 was the highest among three time periods. We inferred that the reason for a more obvious and sharper temperature drop in these two sections could be stronger plant transpiration at noon than 9:00 to 9:30 and 16:00 to 16:30.

4.3. New Insights on the Implications for Landscape and Urban Planning

The findings demonstrated the different effects of different vegetation coverage on thermal comfort in the Laoshan District Coastal Walkway. The results showed that rich vegetation design can beautify the environment and regulate the outdoor thermal environment effectively at the same time; on the other hand, although distinctive structures such as trestle bridges can enrich the landscape of outdoor public spaces such as greenways, they also have a negative impact on the regulation of the outdoor thermal environment. Therefore, these findings provide landscape architects and urban planners to consider the impact of landscape design on outdoor thermal comfort. In future, designers should explore new design strategies to enhance outdoor thermal comfort to make better use of coastal walkways.

4.4. Shortcomings and Outlooks

First, there were still subtle errors despite having fixed the data because mobile measurements require researchers to pay more effort in correcting the GPS data, which have a certain geographic offset. Second, the quick changes in the seaside microclimate interfered with the process of the experiment because the coastal greenway is adjacent to the sea. Finally, long-time and long-distance mobile measurements cannot be performed due to manpower and equipment limitations, so this study selected 1.5 km of the Laoshan District Costal Greenway as a representative sample to carry out the measurements. Moreover, we may add a mini motion camera to the datalogger to record 180-degree panoramic images and videos of the environment during the mobile measurements, and pay more attention to the plant conditions during the survey, in order to find more insights for future experiments. Furthermore, we will explore suitable methods for the measurement of sky visibility factors in narrow linear outdoor spaces such as greenways to explore the influence of spatial morphology on the microclimate of greenways. Nonetheless, the findings of this study can provide a theoretical foundation for future research on the thermal comfort of coastal greenways.

Author Contributions: Conceptualization, R.Z.; data curation, Y.C. and X.Z.; investigation, Y.C., L.Y., X.Z. and Y.L.; methodology, R.Z. and X.M.; project administration, W.G.; supervision, X.M.; validation, L.Y.; writing—original draft, Y.C.; writing—review & editing, R.Z., X.M. and W.G. All authors have read and agreed to the published version of the manuscript.

Funding: This work was funded by the Natural Science Foundation of Shandong Province (China), grant number ZR2020QC172 and the National Natural Science Foundation of China, grant numbers 52008217 and 51908302. The APC was funded by ZR2020QC172.

Institutional Review Board Statement: Not applicable.

Informed Consent Statement: Not applicable.

Data Availability Statement: Not applicable.

Acknowledgments: The authors would like to thank the volunteers (Tian Meng, Fan Wang, Yiping Meng, Liyun Yuan, Danping Xiu, and Weiyi Liu) from the Landscape Architecture Department of the College of Architecture and Urban Planning, Qingdao University of Technology, and the Qingdao citizens for participation in the questionnaire survey related to this work. The authors would also like to thank the associate editor and the reviewers for their useful feedback that improved this paper.

Conflicts of Interest: The authors declare no conflict of interest.

Appendix A

Table A1. The average air temperature (°C), the average relative humidity (%), the average wind speed (m/s), and the average solar radiation (W/m^2) of each section on 11 September and 12 September from 9:00 to 9:30.

Section No.	A	B	C	D	E	F	G	H	I
Average Air Temperature	28.06	27.73	27.93	28.52	28.81	28.76	29.08	28.93	29.05
Average Relative Humidity	78.12	77.97	77.93	76.74	73.58	73.52	73.79	73.42	72.62
Average Wind Speed	0.68	1.18	1.02	0.62	0.35	1.10	0.45	0.60	0.77
Average Solar Radiation	433.93	446.59	577.56	565.49	640.23	578.57	541.14	467.46	518.24

Table A2. The average air temperature (°C), the average relative humidity (%), the average wind speed (m/s), and the average solar radiation (W/m^2) of each section on 11 September and 12 September from 12:00 to 12:30.

Section No.	A	B	C	D	E	F	G	H	I
Average Air Temperature	30.77	30.67	30.35	30.49	29.73	29.82	29.18	29.96	29.71
Average Relative Humidity	69.46	69.75	71.70	69.61	70.67	70.74	74.01	70.78	71.32
Average Wind Speed	0.71	1.14	0.63	0.78	0.75	1.11	1.05	0.80	0.96
Average Solar Radiation	563.23	644.98	617.54	575.71	593.77	559.49	593.53	634.49	625.40

Table A3. The average air temperature (°C), the average relative humidity (%), the average wind speed (m/s), and the average solar radiation (W/m^2) of each section on 11 September and 12 September from 16:00 to 16:30.

Section No.	A	B	C	D	E	F	G	H	I
Average Air Temperature	27.81	27.44	27.47	27.31	27.14	27.15	27.10	27.26	27.38
Average Relative Humidity	78.32	79.26	79.60	79.61	80.47	80.67	81.12	80.48	80.23
Average Wind Speed	0.68	1.18	1.02	0.62	0.35	1.10	0.45	0.60	0.77
Average Solar Radiation	98.91	114.08	130.25	109.93	118.78	140.44	131.77	96.58	111.60

Table A4. Data required for Rayman.

Name of Options in Rayman	Data Content	Detailed Parameters
Data and time	The time and date of the measurement	9:00–9:30, 12:00–12:30, 16:00–16:30; 9.11–9.12, 2021
Geographic data	Latitude, longitude, time zone of the site	121°26′ 31°12′ UTC + 8 Asia/China
Current data	Air temperature, relative humidity, wind speed, solar radiation	Tables A1–A3
Personal data	Height, weight, age, gender	1.75 m, 75 kg, 35, male
Clothing and activity	Clothing thermal resistance, metabolic rate of activities	0.5 80

Notes: Personal data refers to the default value for an adult Chinese male aged 35 years old. Clothing thermal resistance [37] refers to the default value commonly used in summer. Metabolic rate of activities refers to GB/T 18049-2000 “Regulations for PMV and PPD Indices and Thermal Comfort Conditions in Medium Thermal Environments in China”.

Appendix B

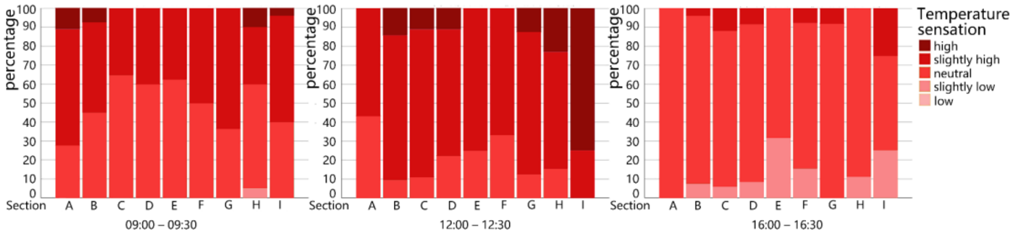

Figure A1. Air temperature sensation votes of the three time periods on 11 September.

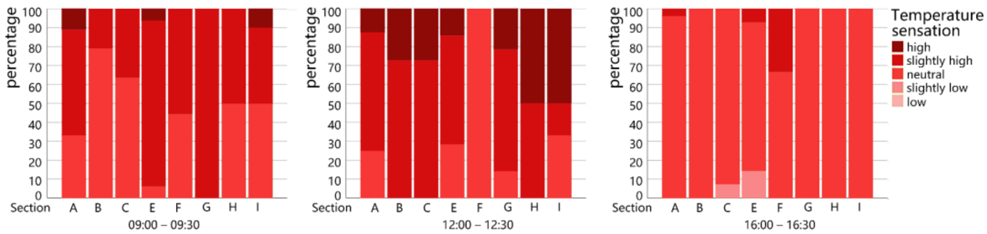

Figure A2. Air temperature sensation votes of the three time periods on 12 September.

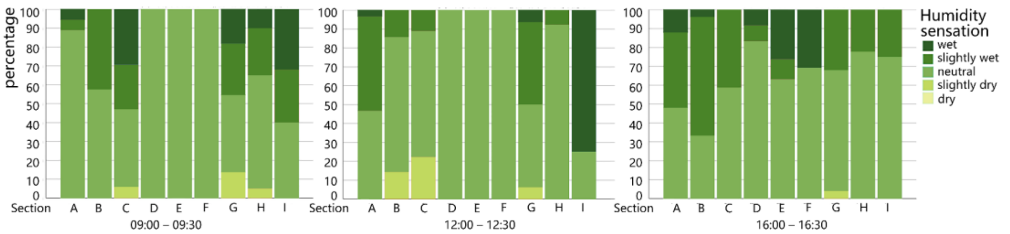

Figure A3. Humidity sensation votes of the three time periods on 11 September.

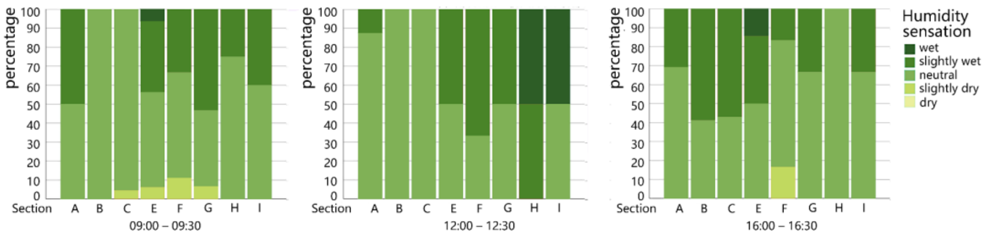

Figure A4. Humidity sensation votes of the three time periods on 12 September.

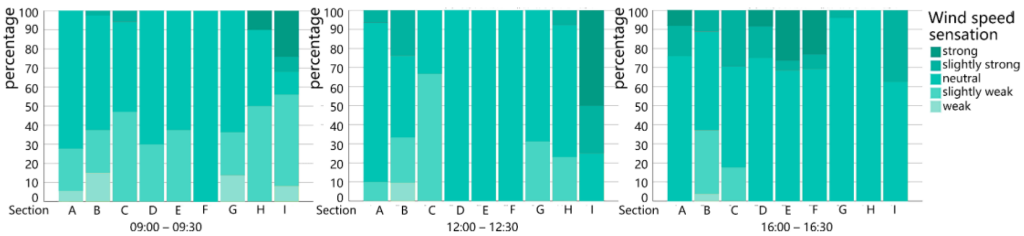

Figure A5. Wind speed sensation votes of the three time periods on 11 September.

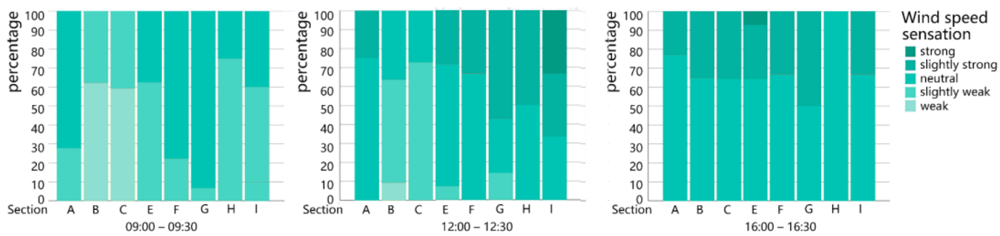

Figure A6. Wind speed sensation votes of the three time periods on 12 September.

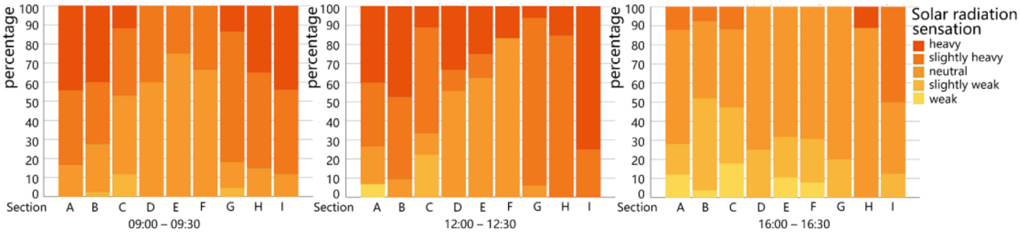

Figure A7. Solar radiation sensation votes of the three time periods on 11 September.

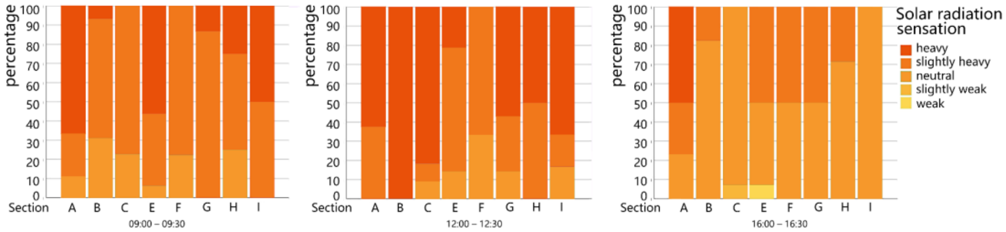

Figure A8. Solar radiation sensation votes of the three time periods on 12 September.

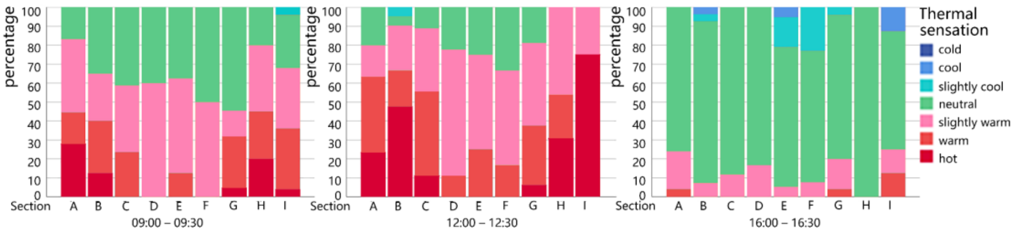

Figure A9. Thermal sensation votes of the three time periods on 11 September.

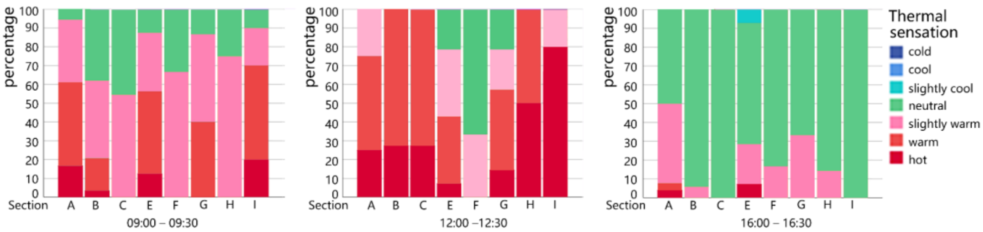

Figure A10. Thermal sensation votes of the three time periods on 12 September.

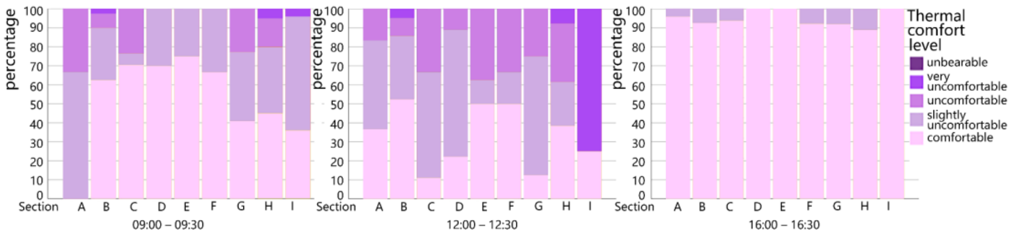

Figure A11. Thermal comfort votes of the three time periods on 11 September.

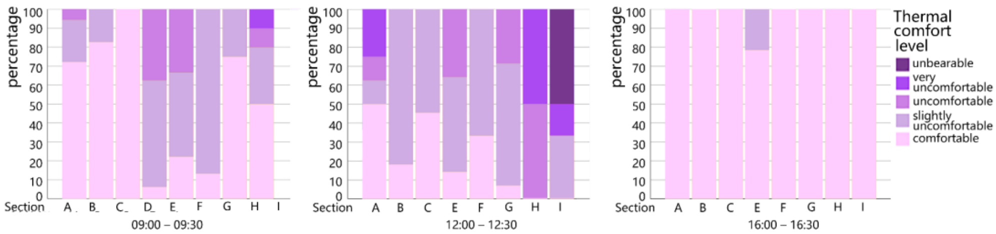

Figure A12. Thermal comfort votes of the three time periods on 12 September.

Appendix C

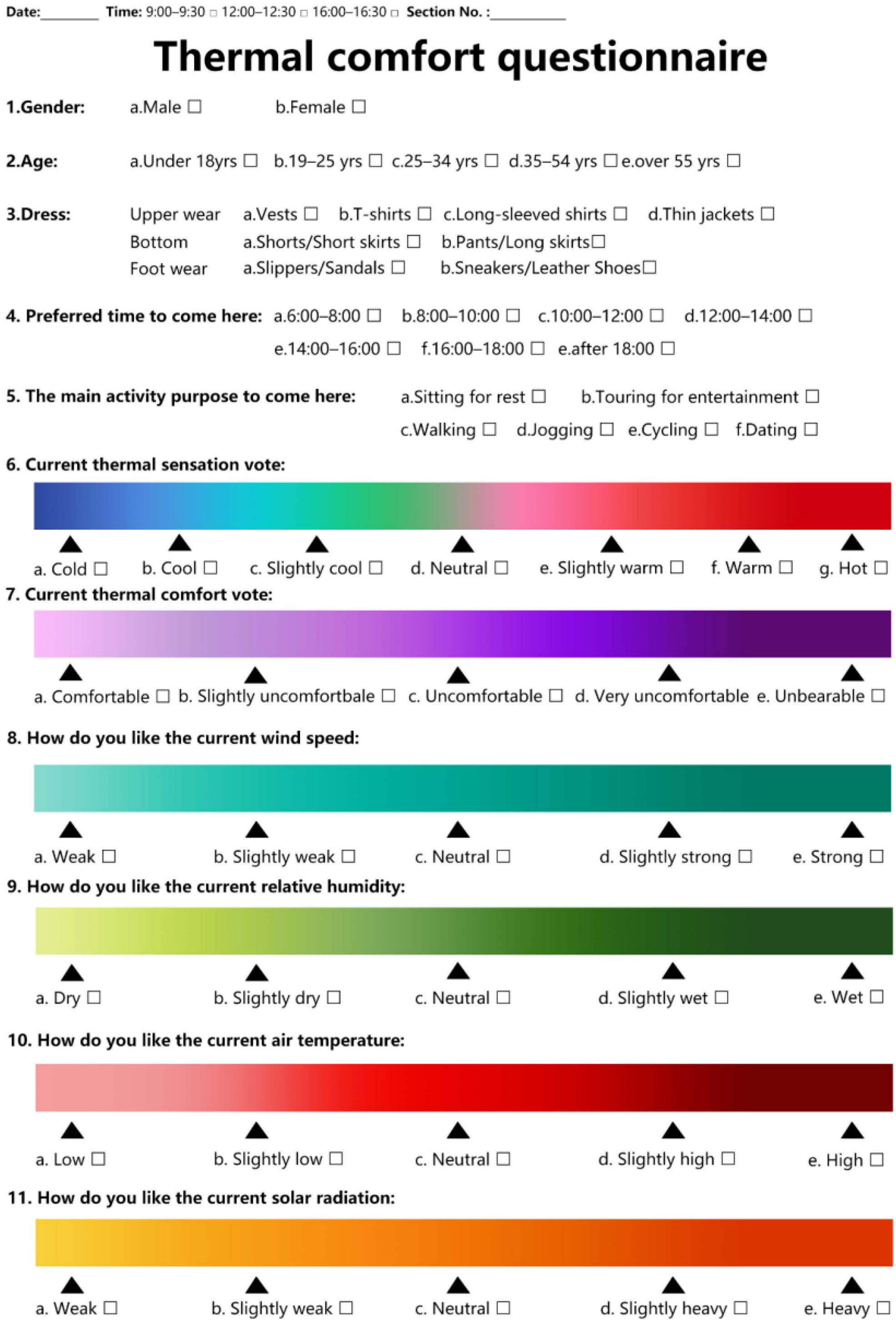

Date:________ Time: 9:00–9:30 □ 12:00–12:30 □ 16:00–16:30 □ Section No. :__________

Thermal comfort questionnaire

1.Gender: a.Male ☐ b.Female ☐

2.Age: a.Under 18yrs ☐ b.19–25 yrs ☐ c.25–34 yrs ☐ d.35–54 yrs ☐ e.over 55 yrs ☐

3.Dress:
Upper wear a.Vests ☐ b.T-shirts ☐ c.Long-sleeved shirts ☐ d.Thin jackets ☐
Bottom a.Shorts/Short skirts ☐ b.Pants/Long skirts☐
Foot wear a.Slippers/Sandals ☐ b.Sneakers/Leather Shoes☐

4. Preferred time to come here: a.6:00–8:00 ☐ b.8:00–10:00 ☐ c.10:00–12:00 ☐ d.12:00–14:00 ☐ e.14:00–16:00 ☐ f.16:00–18:00 ☐ e.after 18:00 ☐

5. The main activity purpose to come here: a.Sitting for rest ☐ b.Touring for entertainment ☐ c.Walking ☐ d.Jogging ☐ e.Cycling ☐ f.Dating ☐

6. Current thermal sensation vote:
a. Cold ☐ b. Cool ☐ c. Slightly cool ☐ d. Neutral ☐ e. Slightly warm ☐ f. Warm ☐ g. Hot ☐

7. Current thermal comfort vote:
a. Comfortable ☐ b. Slightly uncomfortbale ☐ c. Uncomfortable ☐ d. Very uncomfortable e. Unbearable ☐

8. How do you like the current wind speed:
a. Weak ☐ b. Slightly weak ☐ c. Neutral ☐ d. Slightly strong ☐ e. Strong ☐

9. How do you like the current relative humidity:
a. Dry ☐ b. Slightly dry ☐ c. Neutral ☐ d. Slightly wet ☐ e. Wet ☐

10. How do you like the current air temperature:
a. Low ☐ b. Slightly low ☐ c. Neutral ☐ d. Slightly high ☐ e. High ☐

11. How do you like the current solar radiation:
a. Weak ☐ b. Slightly weak ☐ c. Neutral ☐ d. Slightly heavy ☐ e. Heavy ☐

Figure A13. The questionnaire used in the study.

References

1. Manley, G. On the frequency of snowfall in metropolitan England. *Q. J. R. Meteorol. Soc.* **1958**, *84*, 70–72. [CrossRef]
2. Aram, F.; Solgi, E.; Garcia, E.H.; Mosavi, A. Urban heat resilience at the time of global warming: Evaluating the impact of the urban parks on outdoor thermal comfort. *Environ. Sci. Eur.* **2020**, *32*, 1–15. [CrossRef]

3. Wong, L.P.; Alias, H.; Aghamohammadi, N.; Aghazadeh, S.; Sulaiman, N.M.N. Physical, Psychological, and Social Health Impact of Temperature Rise Due to Urban Heat Island Phenomenon and Its Associated Factors. *Biomed. Environ. Sci.* **2018**, *31*, 545–550.
4. Zhu, D.; Zhou, Q.; Liu, M.; Bi, J. Non-optimum temperature-related mortality burden in China: Addressing the dual influences of climate change and urban heat islands. *Sci. Total Environ.* **2021**, *782*, 146760. [CrossRef]
5. Kim, S.; Yoon, S. The Correlation between Outdoor Temperature Distributionand Urban Structure in the Costal City. *Korean Soc. Living Environ. Syst.* **2007**, *14*, 313–319.
6. Marzouk, M.; Attia, K.; Azab, S. Assessment of Coastal Vulnerability to Climate Change Impacts using GIS and Remote Sensing: A Case Study of Al-Alamein New City. *J. Clean. Prod.* **2021**, *290*, 125723. [CrossRef]
7. Yeo, I.; Yee, J.J.; Yoon, S. An Analysis of Urban Temperature and Air-Conditioning Energy Characteristics by Eco-Friendly Urban Planning. *J. Archit. Inst. Korea Plan. Des.* **2010**, *26*, 255–265.
8. Pascal, M.; Goria, S.; Wagner, V.; Sabastia, M.; Guillet, A.; Cordeau, E.; Mauclair, C.; Host, S. Greening is a promising but likely insufficient adaptation strategy to limit the health impacts of extreme heat. *Environ. Int.* **2021**, *151*, 106441. [CrossRef]
9. Huang, H.; Yang, H.; Chen, Y.; Chen, T.; Bai, L.; Peng, Z.R. Urban green space optimization based on a climate health risk appraisal–A case study of Beijing city, China. *Urban For. Urban Green.* **2021**, *62*, 127154. [CrossRef]
10. Marando, F.; Salvatori, E.; Sebastiani, A.; Fusaro, L.; Manes, F. Regulating Ecosystem Services and Green Infrastructure: Assessment of Urban Heat Island effect mitigation in the municipality of Rome, Italy. *Ecol. Model.* **2019**, *392*, 92–102. [CrossRef]
11. Elliott, H.; Eon, C.; Breadsell, J.K. Improving City Vitality through Urban Heat Reduction with Green Infrastructure and Design Solutions: A Systematic Literature Review. *Buildings* **2020**, *10*, 219. [CrossRef]
12. Duan, J.; Wang, Y.; Fan, C.; Xia, B.; De Groot, R. Perception of Urban Environmental Risks and the Effects of Urban Green Infrastructures (UGIs) on Human Well-being in Four Public Green Spaces of Guangzhou, China. *Environ. Manag.* **2018**, *62*, 500–517. [CrossRef] [PubMed]
13. Linehan, J.; Gross, M.; Finn, J. Greenway planning: Developing a landscape ecological network approach. *Landsc. Urban Plan.* **1995**, *33*, 179–193. [CrossRef]
14. Bryant, M.M. Urban landscape conservation and the role of ecological greenways at local and metropolitan scales. *Landsc. Urban Plan.* **2006**, *76*, 23–44. [CrossRef]
15. Smith, D.S.; Hellmund, P.C. *Ecology of Greenways: Design and Function of Linear Conservation Areas*, 1st ed.; University of Minnesota Pr: Minneapolis, MN, USA, 1993.
16. Lee, J.; Kweon, B.-S.; Ellis, C.D.; Lee, S.-W. Assessing the Social Value of Ecosystem Services for Resilient Riparian Greenway Planning and Management in an Urban Community. *Int. J. Environ. Res. Public Health* **2020**, *17*, 3261. [CrossRef]
17. Wu, J.Y. Conservation of Agriculture Landscape through Greenway Planning and Design: A Case Study of the Wax Gourd Production Base of Xiaolou Town, Zengcheng (Guangdong). *Adv. Mater. Res.* **2013**, *869-870*, 235–238. [CrossRef]
18. Wu, J.Y.; Xie, C. Analysis and Evaluation of Guangzhou Zengcheng Greenway. In Proceedings of the 2012 World Automation Congress (WAC), Puerto Vallarta, Mexico, 24–28 June 2012.
19. Hong, L.P.; Hua, X. Greenway as a New Path for the Exploration of Urban-Rural Coordinate based on a Low-Carbon Model: A Case Study of Greenway Planning and Construction in Dongguan, Guangdong province (China). In Proceedings of the 49th Isocarp Congress: Frontiers of Planning—Evolving and Declining Models of Planning Practice, Brisbane, Australia, 1–4 October 2013; pp. 1188–1200.
20. Liu, Z.; Lin, Y.; De Meulder, B.; Wang, S. Can greenways perform as a new planning strategy in the Pearl River Delta, China? *Landsc. Urban Plan.* **2019**, *187*, 81–95. [CrossRef]
21. Chi, W.; Lin, G. The Use of Community Greenways: A Case Study on A Linear Greenway Space in High Dense Residential Areas, Guangzhou. *Land* **2019**, *8*, 188. [CrossRef]
22. Leconte, F.; Bouyer, J.; Claverie, R.; Pétrissans, M. Using Local Climate Zone scheme for UHI assessment: Evaluation of the method using mobile measurements. *Build. Environ.* **2015**, *83*, 39–49. [CrossRef]
23. Stewart, I.D.; Oke, T.R.; Krayenhoff, E.S. Evaluation of the 'local climate zone' scheme using temperature observations and model simulations. *Int. J. Climatol.* **2014**, *34*, 1062–1080. [CrossRef]
24. Sundborg, A. *Climatological Studies in Uppsala with Special Regard to the Temperature Conditions in the Urban Area*; Geographical Institute of Uppsala: Geographica, Japan, 1951.
25. Qaid, A.; Bin Lamit, H.; Ossen, D.R.; Shahminan, R.N.R. Urban heat island and thermal comfort conditions at micro-climate scale in a tropical planned city. *Energy Build.* **2016**, *133*, 577–595. [CrossRef]
26. Zaki, S.; Azid, N.; Shahidan, M.; Hassan, M.; Daud, M.M.; Abu Bakar, N.; Salim, S.A.Z.S.; Yakub, F. Analysis of Urban Morphological Effect on the Microclimate of the Urban Residential Area of Kampung Baru in Kuala Lumpur Using a Geospatial Approach. *Sustainability* **2020**, *12*, 7301. [CrossRef]
27. Tondini, S.; Hasanabadi, F.; Monsorno, R.; Novelli, A. Toward Near Real-Time Kinematics Differential Correction: In View of Geometrically Augmented Sensor Data for Mobile Microclimate Monitoring. *Eng. Proc.* **2020**, *2*, 61.
28. Chan, S.Y.; Chau, C.K. On the study of the effects of microclimate and park and surrounding building configuration on thermal comfort in urban parks. *Sustain. Cities Soc.* **2021**, *64*, 102512. [CrossRef]
29. He, B.-J.; Ding, L.; Prasad, D. Urban ventilation and its potential for local warming mitigation: A field experiment in an open low-rise gridiron precinct. *Sustain. Cities Soc.* **2020**, *55*, 102028. [CrossRef]

30. Höppe, P. The physiological equivalent temperature–A universal index for the biometeorological assessment of the thermal environment. *Int. J. Biometeorol.* **1999**, *43*, 71–75. [CrossRef] [PubMed]
31. Fiala, D.; Havenith, G.; Bröde, P.; Kampmann, B.; Jendritzky, G. UTCI-Fiala multi-node model of human heat transfer and temperature regulation. *Int. J. Biometeorol.* **2011**, *56*, 429–441. [CrossRef] [PubMed]
32. Chen, Q.; Lin, C.; Guo, D.; Hou, Y.; Lai, D. Studies of outdoor thermal comfort in northern China. *Build. Environ.* **2014**, *77*, 110–118. [CrossRef]
33. Huang, J.; Zhou, C.; Zhuo, Y.; Xu, L.; Jiang, Y. Outdoor thermal environments and activities in open space: An experiment study in humid subtropical climates. *Build. Environ.* **2016**, *103*, 238–249. [CrossRef]
34. Fang, Z.; Feng, X.; Liu, A.J.; Lin, Z.; Mak, C.M.; Niu, J.; Tse, K.-T.; Xu, X. Investigation into the differences among several outdoor thermal comfort indices against field survey in subtropics. *Sustain. Cities Soc.* **2019**, *44*, 676–690. [CrossRef]
35. Xu, M.; Hong, B.; Jiang, R.; An, L.; Zhang, T. Outdoor thermal comfort of shaded spaces in an urban park in the cold region of China. *Build. Environ.* **2019**, *155*, 408–420. [CrossRef]
36. Zaki, S.A.; Othman, N.E.; Syahidah, S.W.; Yakub, F.; Muhammad-Sukki, F.; Ardila-Rey, J.A.; Shahidan, M.F.; Saudi, A.S.M. Effects of Urban Morphology on Microclimate Parameters in an Urban University Campus. *Sustainability* **2020**, *12*, 2962. [CrossRef]
37. Matzarakis, A.; Fröhlich, D. Influence of urban green on human thermal bioclimate—Application of thermal indices and micro-scale models. *Acta Hortic.* **2018**, 1–10. [CrossRef]
38. Li, W.; Ouyang, Z.; Meng, X.; Wang, X. Plant species composition in relation to green cover configuration and function of urban parks in Beijing, China. *Ecol. Res.* **2006**, *21*, 221–237. [CrossRef]
39. Pigliautile, I.; Pisello, A. Environmental data clustering analysis through wearable sensing techniques: New bottom-up process aimed to identify intra-urban granular morphologies from pedestrian transects. *Build. Environ.* **2020**, *171*, 106641. [CrossRef]
40. Colter, K.; Middel, A.; Martin, C. Effects of natural and artificial shade on human thermal comfort in residential neighborhood parks of Phoenix, Arizona, USA. *Urban For. Urban Green.* **2019**, *44*, 44. [CrossRef]
41. Davtalab, J.; Deyhimi, S.P.; Dessi, V.; Hafezi, M.R.; Adib, M. The impact of green space structure on physiological equivalent temperature index in open space. *Urban Clim.* **2020**, *31*, 100574. [CrossRef]
42. Ali, S.B.; Patnaik, S. Thermal comfort in urban open spaces: Objective assessment and subjective perception study in tropical city of Bhopal, India. *Urban Clim.* **2018**, *24*, 954–967. [CrossRef]
43. Lin, W.; Zeng, C.; Lam, N.S.-N.; Liu, Z.; Tao, J.; Zhang, X.; Lyu, B.; Li, N.; Li, D.; Chen, Q. Study of the relationship between the spatial structure and thermal comfort of a pure forest with four distinct seasons at the microscale level. *Urban For. Urban Green.* **2021**, *62*, 127168. [CrossRef]
44. Morakinyo, T.E.; Kong, L.; Lau KK, L.; Yuan, C.; Ng, E. A study on the impact of shadow-cast and tree species on in-canyon and neighborhood's thermal comfort. *Build. Environ.* **2017**, *115*, 1–17. [CrossRef]